Hindawi Publishing Corporation
International Journal of Antennas and Propagation
Volume 2015, Article ID 621358, 9 pages
http://dx.doi.org/10.1155/2015/621358

Research Article

Beamspace Unitary ESPRIT Algorithm for Angle Estimation in Bistatic MIMO Radar

Dang Xiaofang, Chen Baixiao, Yang Minglei, and Zheng Guimei

National Laboratory of Radar Signal Processing, Xidian University, Xi'an, Shaanxi 710071, China

Correspondence should be addressed to Dang Xiaofang; xiaofang_dang@sina.cn

Received 28 February 2014; Revised 5 September 2014; Accepted 21 October 2014

Academic Editor: Hang Hu

The beamspace unitary ESPRIT (B-UESPRIT) algorithm for estimating the joint direction of arrival (DOA) and the direction of departure (DOD) in bistatic multiple-input multiple-output (MIMO) radar is proposed. The conjugate centrosymmetrized DFT matrix is utilized to retain the rotational invariance structure in the beamspace transformation for both the receiving array and the transmitting array. Then the real-valued unitary ESPRIT algorithm is used to estimate DODs and DOAs which have been paired automatically. The proposed algorithm does not require peak searching, presents low complexity, and provides a significant better performance compared to some existing methods, such as the element-space ESPRIT (E-ESPRIT) algorithm and the beamspace ESPRIT (B-ESPRIT) algorithm for bistatic MIMO radar. Simulation results are conducted to show these conclusions.

1. Introduction

Multiple-input multiple-output (MIMO) radar [1–6] is developed on the basis of MIMO communication theory, which has gained increasing attention and wide investigation in recent years. MIMO radar can emit orthogonal waveforms simultaneously through multiple antennas and also extract the orthogonal waveforms by using a bank of matched filters. Compared with the traditional phased array radars, a lot of potential advantages of MIMO radars, such as more degrees of freedom (DOFs) [2], better parameter identifiability [2], and higher angular estimation accuracy [3], increasingly appear. According to the configuration of transmitting/receiving arrays, MIMO radars can be grouped into two classes: the former is called statistical MIMO radar, where the transmitting and receiving antennas are widely spaced [1, 3, 4]. It aims at overcoming the radar cross section (RCS) scintillation effect which was encountered in radar systems by capitalizing on the spatial diversity [5]. The latter is known as monostatic MIMO radar or bistatic MIMO radar [2, 6–10], where the transmitting and receiving antennas are closely spaced. Monostatic or bistatic MIMO radar, which can form receiving beam and virtual transmitting beam jointly at the receiver [2], has many advantages, such as narrower beamwidth, lower sidelobes, higher angular resolution, and higher angular estimation accuracy [6, 11]. And this paper focuses on the bistatic MIMO radar.

For the bistatic MIMO radar, one of the most important issues is to estimate the directions of departure and arrival of multiple targets from the received signals corrupted by noise. So far various approaches have been put forward. In [7], the two-dimensional (2D) Capon estimator is introduced to estimate the DOAs and the DODs of the targets in bistatic MIMO radar. To reduce the computational cost, a polynomial rooting estimator is introduced in [8]. The 2D multiple signal classification (MUSIC) algorithm and reduced-dimension MUSIC (RD-MUSIC) algorithm are discussed in [12, 13]. To alleviate the computational burden, the ESPRIT algorithm [14] is used for target direction estimation by utilizing the invariance property of both the transmitting array and the receiving array. Nevertheless, an additional matched pair is required in the ESPRIT algorithm. In order to solve this problem, a unitary ESPRIT algorithm for bistatic MIMO radar is proposed in [15], which fully exploits the real-valued rotational invariance equations of signal subspace to estimate DODs and DOAs that are paired automatically. When some a priori knowledge of the angle information of sources is known, the beamspace ESPRIT (B-ESPRIT) [16] algorithm

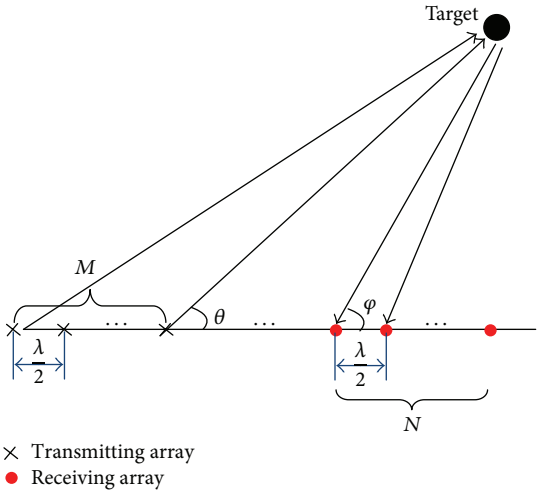

Figure 1: The configuration of bistatic MIMO radar.

is raised to reduce computational complexity; however, an additional pair matching is also needed and a degradation of the algorithm's performance can be observed as well.

To overcome the aforementioned problems, a beamspace unitary ESPRIT algorithm is developed to estimate DODs and DOAs of the targets in bistatic MIMO radar in this paper. First, the conjugate centrosymmetrized DFT matrix is employed to retain the rotational invariance structure in the beamspace transformation for both the receiving array and the transmitting array. Then the DODs and DOAs can be estimated in accordance with a new version of ESPRIT for the bistatic MIMO radar. The ESPRIT algorithm works in the beamspace and involves only real-valued computation from start to finish. Over the beamspace ESPRIT algorithm, the proposed algorithm has better performance that can be paired automatically for DODs and DOAs estimation. In some situation, the proposed algorithm also has a better performance over the element ESPRIT.

And the structure of the rest of the paper will be organized as follows. The bistatic MIMO radar signal model is presented in Section 2. The proposed beamspace unitary ESPRIT for DODs and DOAs estimation is proposed in Section 3. Section 4 gives the computational complexity analysis of the proposed algorithm, unitary ESPRIT, and beamspace ESPRIT; advantages and disadvantages of the proposed algorithm also have been discussed in Section 4. And simulation results are provided to verify the performance of the proposed algorithm in Section 5; the Cramer-Rao Bound (CRB) also has been derived in this section. Finally, Section 6 concludes this paper.

2. Signal Model of the Bistatic MIMO Radar

Considering a narrowband bistatic MIMO radar system with an M-element transmitting array and an N-element receiving array, we found that both are half-wave length spaced uniform linear arrays (Figure 1).

At the transmitting site, M different orthogonal narrowband waveforms are emitted simultaneously. In each receiver, the echoes are processed for all of the transmitted waveforms. Assume that there are P uncorrelated targets in the same range bin, located in the far field of the array. The DOD and DOA of the pth target with respect to the transmitting array and the receiving array are denoted by θ_p and φ_p, respectively. Thus, the output of all the matched filters in receivers can be written as

$$\mathbf{X}(t) = \mathbf{A}\mathbf{S}(t) + \mathbf{N}(t), \tag{1}$$

where $\mathbf{A} = [\mathbf{a}_1, \mathbf{a}_2, \ldots, \mathbf{a}_p]$ is an $MN \times P$ matrix, the column vectors $\mathbf{a}_p$, $p = 1, \ldots, P$ are P steering vectors, which can be written as $\mathbf{a}_p = \mathbf{a}_r(\mu_p) \otimes \mathbf{a}_t(\nu_p)$, is the combined steering vector of pth target, where $\mathbf{a}_r(\mu_p) = \begin{bmatrix} 1 & e^{j\mu_p} & \cdots & e^{j(N-1)\mu_p} \end{bmatrix}^T \in C^{N\times 1}$ and $\mathbf{a}_t(\nu_p) = \begin{bmatrix} 1 & e^{j\nu_p} & \cdots & e^{j(M-1)\nu_p} \end{bmatrix}^T \in C^{M\times 1}$ are the receiving and transmitting steering vector of the pth target, and $\mu_p = \pi \sin\varphi_p$ and $\nu_p = \pi \sin\theta_p$, respectively; $\otimes$ denotes the Kronecker product; $\mathbf{S}(t) = \begin{bmatrix} s_1(t) & s_2(t) & \cdots & s_P(t) \end{bmatrix}^T$ is a column vector consisted of the amplitudes and phases of the P sources at time t; $s_p(t)$ is usually in the form of $s_p(t) = \alpha_p e^{j\omega_p t}$ with α_p being the complex amplitude and ω_p the Doppler frequency of the pth target; $\mathbf{N}(t)$ is the additive noise, which is modeled as a zero-mean, spatially white Gaussian process with covariance matrix $\sigma_n^2 \mathbf{I}_{MN}$, where $\mathbf{I}_{MN}$ denotes an $MN \times MN$ identity matrix.

Note that the dimension of $\mathbf{X}$ will be $MN \times J$, and J is the number of time samples. When M and N are large, the computational load and time will be huge. To overcome this shortcoming, the beamspace unitary ESPRIT is proposed as follows.

3. Proposed Method for DOD and DOA Estimation

In a radar application, the operation of reducing dimension could be facilitated in beamspace when a priori information on the general angular locations of the signal arrivals presents. In this case, by utilizing the beamspace transform matrix, beams, which involve the sector of interest, would be formed, thereby reducing computational complexity. And if there is no a priori information, one may apply angle estimation algorithm via parallel processing to each of the number of sets of successive overlapped sectors, which will also reduce computational complexity.

To retain the rotational invariance structure in the beamspace transformation, in this paper, the conjugate centrosymmetrized DFT matrix is applied as the beamspace transformed matrix. Let $\mathbf{W}_r^H$ be the receiving beamspace transformed matrix and let $\mathbf{W}_t^H$ be the transmitting

beamspace transformed matrix. The mth row of $\mathbf{W}_r^H$ and $\mathbf{W}_t^H$ is formulated as [17]

$$\begin{aligned}\mathbf{w}_{r,m}^H &= e^{j((N-1)/2)m(2\pi/N)} \\ &\quad \cdot \left[1, e^{-jm(2\pi/N)}, \ldots, e^{-j(N-1)m(2\pi/N)}\right], \\ &\qquad m = 0, \ldots, N-1 \\ \mathbf{w}_{t,m}^H &= e^{j((M-1)/2)m(2\pi/M)} \\ &\quad \cdot \left[1, e^{-jm(2\pi/M)}, \ldots, e^{-j(M-1)m(2\pi/M)}\right], \\ &\qquad m = 0, \ldots, M-1.\end{aligned} \tag{2}$$

Both $\mathbf{W}_r^H$ and $\mathbf{W}_t^H$ are conjugate centrosymmetrized matrixes and their mth row vector represents a DFT beam steered at the spatial frequency $\mu = m(2\pi/N)$ and $\nu = m(2\pi/M)$, respectively. An important property of the Kronecker operator that will prove useful throughout the transformation is

$$(\mathbf{A} \otimes \mathbf{B})(\mathbf{C} \otimes \mathbf{D}) = \mathbf{AC} \otimes \mathbf{BD}, \tag{3}$$

where $\mathbf{A}$ is an $m \times n$ matrix, which is not the matrix $\mathbf{A}$ mentioned above in (1). $\mathbf{B}$ is a $p \times q$ matrix, which is also not the matrix $\mathbf{B}$ mentioned below in (5). $\mathbf{C}$ is an $n \times r$ matrix and $\mathbf{D}$ is a $q \times s$ matrix.

The receiving beamspace manifold is defined as $\mathbf{B}_r = \mathbf{W}_r^H \mathbf{A}_r$ and the transmitting beamspace manifold is defined as $\mathbf{B}_t = \mathbf{W}_t^H \mathbf{A}_t$, respectively. Then the final beamspace manifold can be written as

$$\begin{aligned}\mathbf{B} &= \mathbf{W}^H \mathbf{A} = \mathbf{B}_r \otimes \mathbf{B}_t \\ &= \mathbf{W}_r^H \mathbf{A}_r \otimes \mathbf{W}_t^H \mathbf{A}_t.\end{aligned} \tag{4}$$

According to property (3), the equation $\mathbf{W}_r^H \mathbf{A}_r \otimes \mathbf{W}_t^H \mathbf{A}_t = (\mathbf{W}_r^H \otimes \mathbf{W}_t^H)(\mathbf{A}_r \otimes \mathbf{A}_t)$ holds. Thus, the final beamspace transformed matrix is defined as

$$\mathbf{W}^H = \mathbf{W}_r^H \otimes \mathbf{W}_t^H. \tag{5}$$

$\mathbf{W}$ is an $K_t K_r \times MN$ matrix, where K_t and K_r are the number of transmitting beam and receiving beam, respectively. A new beamspace received signal is defined as

$$\begin{aligned}\mathbf{Y}(t) &= \mathbf{W}^H \mathbf{A}\mathbf{S}(t) + \overline{\mathbf{N}}(t) \\ &= \mathbf{B}\mathbf{S}(t) + \overline{\mathbf{N}}(t),\end{aligned} \tag{6}$$

where $\overline{\mathbf{N}}(t) = \mathbf{W}^H \mathbf{N}(t)$ is the noise of beamspace.

Next the rotational invariance structure in the beamspace will be examined. Considering the receiving beamspace manifold $\mathbf{B}_r = [\mathbf{b}_r(\mu_1), \ldots, \mathbf{b}_r(\mu_P)]$, the pth component of $\mathbf{B}_r$ is $\mathbf{b}_r(\mu_p) = [b_{r,0}(\mu_p), \ldots, b_{r,N-1}(\mu_p)]^T$. And the mth elements of $\mathbf{b}_r(\mu_p)$ are

$$b_{r,m}(\mu_p) = \mathbf{w}_{r,m}^H \mathbf{a}_r(\mu) = \frac{\sin\left[(N/2)\left(\mu_p - m(2\pi/N)\right)\right]}{\sin\left[(1/2)\left(\mu_p - m(2\pi/N)\right)\right]}. \tag{7}$$

Comparing (7) with $b_{r,m+1}(\mu_p)$, it is observed that the numerator of $b_{r,m+1}(\mu_p)$ is the negative of that of $b_{r,m}(\mu_p)$. Then the two adjacent components of $\mathbf{b}_r(\mu_p)$ are related as [18]

$$\begin{aligned}&\sin\left[\frac{1}{2}\left(\mu_p - m\frac{2\pi}{N}\right)\right] b_{r,m}(\mu_p) \\ &\quad + \sin\left[\frac{1}{2}\left(\mu_p - (m+1)\frac{2\pi}{N}\right)\right] b_{r,m+1}(\mu_p) = 0.\end{aligned} \tag{8}$$

Trigonometric equations lead to

$$\begin{aligned}&\tan\left(\frac{\mu_p}{2}\right)\left\{\cos\left(m\frac{\pi}{N}\right) b_{r,m}(\mu_p)\right. \\ &\qquad \left. + \cos\left((m+1)\frac{\pi}{N}\right) b_{r,m+1}(\mu_p)\right\} \\ &= \sin\left(m\frac{\pi}{N}\right) b_{r,m}(\mu_p) + \sin\left((m+1)\frac{\pi}{N}\right) b_{r,m+1}(\mu_p).\end{aligned} \tag{9}$$

Due to the fact that the beams with indices $m = 0$ and $m = N-1$ are steered at the spatial frequencies $\mu_{p,0} = 0$ and $\mu_{p,N-1} - 2\pi = (N-1)(2\pi/N) - 2\pi = -2\pi/N$, where the two beams are physically adjacent to each other. First, we observe that

$$\begin{aligned}b_N(\mu_p) &= \frac{\sin\left[(N/2)\left(\mu_p - N(2\pi/N)\right)\right]}{\sin\left[(1/2)\left(\mu_p - N(2\pi/N)\right)\right]} \\ &= \frac{\sin\left((N/2)\mu_p - N\pi\right)}{\sin\left((1/2)\mu_p - \pi\right)} \\ &= \frac{(-1)^N \sin\left((N/2)\mu_p\right)}{-\sin\left((1/2)\mu_p\right)} = (-1)^{N-1} \cdot b_0(\mu_p).\end{aligned} \tag{10}$$

Then, the first and the last elements of $\mathbf{b}_r(\mu_p)$ are related by setting $m = N-1$ in (9), and there is

$$\begin{aligned}&\tan\left(\frac{\mu_p}{2}\right)\left\{\cos\left((N-1)\frac{\pi}{N}\right) b_{r,N-1}(\mu_p)\right. \\ &\qquad \left. + \cos(\pi)(-1)^{(N-1)} b_{r,0}(\mu_p)\right\} \\ &= \sin\left((N-1)\frac{\pi}{N}\right) b_{r,N-1}(\mu_p) \\ &\quad + \sin(\pi)(-1)^{(N-1)} b_{r,0}(\mu_p).\end{aligned} \tag{11}$$

All N equations ($0 \le m \le N-1$) lead to an invariance relationship for the $\mathbf{b}_r(\mu_p)$ as follows:

$$\tan\left(\frac{\mu_p}{2}\right) \mathbf{\Gamma}_1 \mathbf{b}_r(\mu_p) = \mathbf{\Gamma}_2 \mathbf{b}_r(\mu_p), \tag{12}$$

where $\mathbf{\Gamma}_1$ and $\mathbf{\Gamma}_2$ are the two selection matrices defined as

$$\boldsymbol{\Gamma}_1 = \begin{bmatrix} 1 & \cos\left(\frac{\pi}{N}\right) & 0 & 0 & \cdots & 0 & 0 \\ 0 & \cos\left(\frac{\pi}{N}\right) & \cos\left(\frac{2\pi}{N}\right) & 0 & \cdots & 0 & 0 \\ 0 & 0 & \cos\left(\frac{2\pi}{N}\right) & \cos\left(\frac{3\pi}{N}\right) & \cdots & 0 & 0 \\ \vdots & \vdots & \vdots & \vdots & \cdot & \vdots & \vdots \\ 0 & 0 & 0 & 0 & \cdots & \cos\left((N-2)\frac{\pi}{N}\right) & \cos\left((N-1)\frac{\pi}{N}\right) \\ (-1)^N & 0 & 0 & 0 & \cdots & 0 & \cos\left((N-1)\frac{\pi}{N}\right) \end{bmatrix},$$

$$\boldsymbol{\Gamma}_2 = \begin{bmatrix} 0 & \sin\left(\frac{\pi}{N}\right) & 0 & 0 & \cdots & 0 & 0 \\ 0 & \sin\left(\frac{\pi}{N}\right) & \sin\left(\frac{2\pi}{N}\right) & 0 & \cdots & 0 & 0 \\ 0 & 0 & \sin\left(\frac{2\pi}{N}\right) & \sin\left(\frac{3\pi}{N}\right) & \cdots & 0 & 0 \\ \vdots & \vdots & \vdots & \vdots & \cdot & \vdots & \vdots \\ 0 & 0 & 0 & 0 & \cdots & \sin\left((N-2)\frac{\pi}{N}\right) & \sin\left((N-1)\frac{\pi}{N}\right) \\ 0 & 0 & 0 & 0 & \cdots & 0 & \sin\left((N-1)\frac{\pi}{N}\right) \end{bmatrix}. \tag{13}$$

When some a priori knowledge of the angle information of sources is known, a reduced dimension processing can be achieved by applying a subset of row vectors defined in (4) to the data matrix $\mathbf{X}$. Hence, only those subblocks of the selection matrices $\boldsymbol{\Gamma}_1$ and $\boldsymbol{\Gamma}_2$ which are correlated with the corresponding components of $\mathbf{b}_r(\mu_p)$ will be used.

With P targets, (12) translates into the receiving beamspace matrix relation:

$$\boldsymbol{\Gamma}_1 \mathbf{B}_r \boldsymbol{\Omega}_\mu = \boldsymbol{\Gamma}_2 \mathbf{B}_r, \tag{14}$$

where $\boldsymbol{\Omega}_\mu = \operatorname{diag}\{\tan(\mu_1/2), \ldots, \tan(\mu_P/2)\}$ is a real-valued diagonal matrix whose diagonal elements contain the desired DOA information. Similar to the relation of receiving beamspace matrix, the relation of transmit beamspace matrix is

$$\boldsymbol{\Gamma}_3 \mathbf{B}_t \boldsymbol{\Omega}_\nu = \boldsymbol{\Gamma}_4 \mathbf{B}_t, \tag{15}$$

where $\boldsymbol{\Gamma}_3$ and $\boldsymbol{\Gamma}_4$ are defined similar to (13) with N replaced by M and $\boldsymbol{\Omega}_\nu = \operatorname{diag}\{\tan(\nu_1/2), \ldots, \tan(\nu_P/2)\}$ is a real-valued diagonal matrix whose diagonal elements contain the desired DOD information.

According to the use of the property of the Kronecker operator in (3), we find that the whole beamspace manifold $\mathbf{B}$ satisfies

$$\begin{aligned} \boldsymbol{\Gamma}_{\mu_1} \mathbf{B} \boldsymbol{\Omega}_\mu &= \boldsymbol{\Gamma}_{\mu_2} \mathbf{B} \\ \boldsymbol{\Gamma}_{\nu_1} \mathbf{B} \boldsymbol{\Omega}_\nu &= \boldsymbol{\Gamma}_{\nu_2} \mathbf{B}, \end{aligned} \tag{16}$$

where $\boldsymbol{\Gamma}_{\mu_1} = \boldsymbol{\Gamma}_1 \otimes \mathbf{I}_M$ and $\boldsymbol{\Gamma}_{\mu_2} = \boldsymbol{\Gamma}_2 \otimes \mathbf{I}_M$ are the receiving beamspace selection matrices and $\boldsymbol{\Gamma}_{\nu_1} = \mathbf{I}_N \otimes \boldsymbol{\Gamma}_3$ and $\boldsymbol{\Gamma}_{\nu_2} = \mathbf{I}_N \otimes \boldsymbol{\Gamma}_4$ are the transmitting beamspace selection matrices, respectively.

Looking back on the beamspace received signal $\mathbf{Y}(t)$ defined in (5), the proper $NM \times P$ matrix of signal subspace for the proposed algorithm can be formed by P "largest" left singular vectors of the real-valued matrix $[\operatorname{Re}(\mathbf{Y}), \operatorname{Im}(\mathbf{Y})]$. As we know, the signal subspace $\mathbf{E}_s$ may be spanned by $\mathbf{B}$, which is expressed as

$$\mathbf{E}_s = \mathbf{B}\mathbf{T}, \tag{17}$$

where $\mathbf{T}$ is an unknown $P \times P$ real-valued matrix. Substituting $\mathbf{B} = \mathbf{E}_s \mathbf{T}^{-1}$ into (16) yields

$$\begin{aligned} \boldsymbol{\Gamma}_{\mu_1} \mathbf{E}_s \boldsymbol{\Psi}_\mu &= \boldsymbol{\Gamma}_{\mu_2} \mathbf{E}_s, \\ \boldsymbol{\Gamma}_{\nu_1} \mathbf{E}_s \boldsymbol{\Psi}_\nu &= \boldsymbol{\Gamma}_{\nu_2} \mathbf{E}_s, \end{aligned} \tag{18}$$

where $\boldsymbol{\Psi}_\mu = \mathbf{T}^{-1} \boldsymbol{\Omega}_\mu \mathbf{T}$ and $\boldsymbol{\Psi}_\nu = \mathbf{T}^{-1} \boldsymbol{\Omega}_\nu \mathbf{T}$. Equation (18) can be solved by the least squares (LS) or the total least squares (TLS) algorithm. Note the fact that all of the quantities of $\boldsymbol{\Psi}_\mu$ and $\boldsymbol{\Psi}_\nu$ are real-valued. Automatic pairing of the spatial frequency μ and ν estimation can be obtained by decomposing $\boldsymbol{\Psi}_\mu + j\boldsymbol{\Psi}_\nu$ as follows:

$$\boldsymbol{\Psi}_\mu + j\boldsymbol{\Psi}_\nu = \mathbf{T}^{-1} \left\{ \boldsymbol{\Omega}_\mu + j\boldsymbol{\Omega}_\nu \right\} \mathbf{T}. \tag{19}$$

Hence, the real and imaginary parts of the eigenvalues $\{\mathbf{\Omega}_\mu + j\mathbf{\Omega}_\nu\}$ are the estimation of $\{\mu_p, \nu_p\}$, $p = 1, \ldots, P$. Then the DODs and DOAs of targets can be derived as follows:

$$\widehat{\theta}_p = \arcsin\left\{\frac{2\arctan\left[\mathbf{\Omega}_\nu\right]_p}{\pi}\right\}, \quad p = 1, \ldots, P,$$
$$\widehat{\varphi}_p = \arcsin\left\{\frac{2\arctan\left[\mathbf{\Omega}_\mu\right]_p}{\pi}\right\}, \quad p = 1, \ldots, P. \tag{20}$$

The beamspace unitary ESPRIT algorithm based on this development is summarized below.

(1) To form the beamspace transformed matrix $\mathbf{W}^H = \mathbf{W}_r^H \otimes \mathbf{W}_t^H$, where $\mathbf{W}^H \in K_t K_r \times MN$.

(2) To transform the receiving data $\mathbf{X}(t)$ into beamspace $\mathbf{Y} = \mathbf{W}^H\mathbf{X}$, where $\mathbf{Y} \in K_t K_r \times J$, J is the number of time samples.

(3) To compute the SVD of $[\mathrm{Re}(\mathbf{Y}), \mathrm{Im}(\mathbf{Y})]$. The P dominant left singular vectors will be called $\mathbf{E}_s \in K_t K_r \times P$. And if P is not known as the a priori information, the number of sources P should be estimated [19].

(4a) To compute $\mathbf{\Psi}_\mu$ by solving the overdetermined system of equation $\mathbf{\Gamma}_{\mu_1}\mathbf{E}_s\mathbf{\Psi}_\mu = \mathbf{\Gamma}_{\mu_2}\mathbf{E}_s$ via the least squares or the total least squares algorithm. The selection matrices $\mathbf{\Gamma}_{\mu_1} = \mathbf{\Gamma}_1 \otimes \mathbf{I}_M$ and $\mathbf{\Gamma}_{\mu_2} = \mathbf{\Gamma}_2 \otimes \mathbf{I}_M$, where $\mathbf{\Gamma}_1$ and $\mathbf{\Gamma}_2$ are defined in (13). When one has the a priori information on the general angular locations of the signal arrivals, only the appropriate subblocks of $\mathbf{\Gamma}_1$ and $\mathbf{\Gamma}_2$ are employed.

(4b) To compute $\mathbf{\Psi}_\nu$ by solving the overdetermined system of equation $\mathbf{\Gamma}_{\nu_1}\mathbf{E}_s\mathbf{\Psi}_\nu = \mathbf{\Gamma}_{\nu_2}\mathbf{E}_s$ by the least squares or the total least squares algorithm. The selection matrices are $\mathbf{\Gamma}_{\nu_1} = \mathbf{I}_N \otimes \mathbf{\Gamma}_3$ and $\mathbf{\Gamma}_{\nu_2} = \mathbf{I}_N \otimes \mathbf{\Gamma}_4$.

(5) To compute the eigendecomposition of matrix $\mathbf{\Psi}_\mu + j\mathbf{\Psi}_\nu$. Then P largest eigenvalues λ_p, $p = 1, \ldots, P$ could be obtained as $\lambda_p = \{[\mathbf{\Omega}_\nu]_p + j[\mathbf{\Omega}_\mu]_p\}$, where $[\mathbf{\Omega}_\nu]_p$ and $[\mathbf{\Omega}_\mu]_p$ are the real and imaginary parts of λ_p, respectively.

(6) To compute the DODs and DOAs as the solution to $\widehat{\theta}_p = \arcsin\{2\arctan[\mathbf{\Omega}_\nu]_p/\pi\}$, $p = 1, \ldots, P$ and $\widehat{\varphi}_p = \arcsin\{2\arctan[\mathbf{\Omega}_\mu]_p/\pi\}$, $p = 1, \ldots, P$ which are paired automatically.

4. Computational Complexity Analysis

In Table 1, the beamspace unitary ESPRIT is compared against the unitary ESPRIT and the beamspace ESPRIT algorithm in terms of computational complexity. For the element ESPRIT and the unitary ESPRIT algorithm, the computational complexity of eigendecomposition is $O(M^3N^3)$, which is very heavy. Unlike the element ESPRIT and the unitary ESPRIT algorithm, the beamspace ESPRIT and the beamspace unitary ESPRIT algorithm transform the original data vector into several lower-dimensional beamspaces. Since the data processing of each beamspace is independent, it can be parallel processed. If only $K_t < M$ transmitting beams and $K_r < N$ receiving beams are selected, the computational complexity could be reduced from $O(M^3N^3)$ to $O(K_t^3K_r^3)$. It is noted that the computational saving is quite significant. Comparing the beamspace unitary ESPRIT with the beamspace ESPRIT algorithm, the proposed algorithm involves only real-valued computation from start to finish. So the computational complexity of beamspace unitary ESPRIT is slightly lower than the beamspace ESPRIT algorithm. And the beamspace unitary ESPRIT algorithm can estimate DOAs and DODs that are paired automatically, which need to be paired additionally in the beamspace ESPRIT algorithm, to save computational complexity.

4.1. Advantages and Disadvantages of the Proposed Algorithm. The proposed algorithm has the following advantages.

(1) The proposed algorithm involves only real-valued computation after the initial transformation of beamspace.

(2) The proposed algorithm has a low complexity for the fact that peak searching is not required. And when a priori information is known, only several beams encompassing the sector of interest need to be formed, thereby yielding further reduced computational complexity.

(3) The proposed algorithm can obtain automatically paired DOD and DOA angle estimations.

(4) The proposed algorithm has a better angle estimation performance than B-ESPRIT algorithm which has been explained in the following section.

The proposed algorithm also has the following disadvantages.

(1) The proposed algorithm shows that, due to the dramatic reduction in computational complexity, the performance degradation would appear.

(2) The proposed algorithm is sensitive to array errors. The rotational invariance structure will be damaged in the presence of array errors.

5. Simulation Results

In this section, some numerical examples are presented to assess the effectiveness of the proposed method. In all

Table 1: Comparison of computational complexities of the beamspace unitary ESPRIT, the beamspace ESPRIT, and the unitary ESPRIT.

Algorithms	Beamspace transformation	Subspace decomposition	DOA and DOD estimation
The unitary ESPRIT	None	$O(M^3N^3)$	$O(2^3P^3)$
The beamspace ESPRIT	$O(JK_tK_rMN)$	$O(K_t^3K_r^3)$	$O(2^3P^3)$
The beamspace unitary ESPRIT	$O(JK_tK_rMN)$	$O(K_t^3K_r^3)$	$O(P^3)$

simulations, 2000 Monte Carlo trials are performed. The RMSE is defined as

$$\text{RMSE}_t = \frac{1}{P}\sum_{p=1}^{P}\sqrt{\frac{1}{1,000}\sum_{l=1}^{1,000}\left(\widehat{\theta}_{p,l}-\theta_p\right)^2},$$

$$\text{RMSE}_r = \frac{1}{P}\sum_{p=1}^{P}\sqrt{\frac{1}{1,000}\sum_{l=1}^{1,000}\left(\widehat{\varphi}_{p,l}-\varphi_p\right)^2},$$

$$\text{RMSE} = \frac{1}{P}\sum_{p=1}^{P}\sqrt{\frac{1}{1,000}\sum_{l=1}^{1,000}\left[\left(\widehat{\theta}_{p,l}-\theta_p\right)^2+\left(\widehat{\varphi}_{p,l}-\varphi_p\right)^2\right]}, \tag{21}$$

which are employed as the performance metric, where θ_p and φ_p denote the DOD and DOA of the pth source and $\widehat{\theta}_{p,l}$ and $\widehat{\varphi}_{p,l}$ are the estimation of θ_p and φ_p in the lth Monte Carlo trail, respectively. J denotes the number of snapshots. According to [16], the CRB for the angle estimation in bistatic MIMO radar is derived as follows:

$$\text{CRB}(\theta,\varphi) = \frac{\sigma^2}{2K}\left\{\text{Re}\left[\mathbf{D}^H\boldsymbol{\Pi}_{\mathbf{B}}^{\perp}\mathbf{D}\odot\widehat{\mathbf{P}}_{SS}^{T}\right]\right\}^{-1}, \tag{22}$$

where $\mathbf{D} = [\partial\mathbf{b}_1/\partial\theta_1, \partial\mathbf{b}_2/\partial\theta_2, \ldots, \partial\mathbf{b}_P/\partial\theta_P, \partial\mathbf{b}_1/\partial\varphi_1, \partial\mathbf{b}_2/\partial\varphi_2, \ldots, \partial\mathbf{b}_P/\partial\varphi_P]$ with $\mathbf{b}_p$ being the pth column of $\mathbf{B}$, $\boldsymbol{\Pi}_{\mathbf{B}}^{\perp} = \mathbf{I}_{MN} - \mathbf{B}(\mathbf{B}^H\mathbf{B})^{-1}\mathbf{B}^H$, $\widehat{\mathbf{P}}_{SS}^{T} = \begin{bmatrix}\widehat{\mathbf{P}}_S & \widehat{\mathbf{P}}_S\\ \widehat{\mathbf{P}}_S & \widehat{\mathbf{P}}_S\end{bmatrix}$, $\widehat{\mathbf{P}}_S = (1/J)\sum_{t=1}^{J}\mathbf{S}(t)\mathbf{S}^H(t)$, σ^2 stands for the noise variance, and J is the number of time samples.

Assuming that there are $P = 3$ sources, whose angles are $(\theta_1,\varphi_1) = (30^\circ,-30^\circ)$, $(\theta_2,\varphi_2) = (20^\circ,-40^\circ)$, and $(\theta_3,\varphi_3) = (40^\circ,-36^\circ)$. For the B-ESPRIT and the proposed algorithm, there are five beams are formed, which involve the sector of interest.

Figures 2 and 3 depict the DOD and DOA estimation results of the proposed algorithm for the three sources in bistatic MIMO radar with $M = 8$, $N = 6$, $J = 64$, SNR = 15 dB, and 20 dB, respectively. It shows that the DODs and DOAs of sources can be clearly observed, and the performance will be improved as the SNR increases.

The proposed algorithm is compared against the beamspace ESPRIT algorithm, the element ESPRIT algorithm, the unitary ESPRIT, and CRB. And in this Simulation, a new source located at $(\theta_4,\varphi_4) = (36^\circ,-36^\circ)$ is added. Figures 4 and 5 present angle estimation performance comparison with $M = 8$, $N = 6$, and $J = 64$. It can be found that the angle estimation performance of proposed algorithm is better than the B-ESPRIT algorithm because unitary ESPRIT doubles the number of data samples

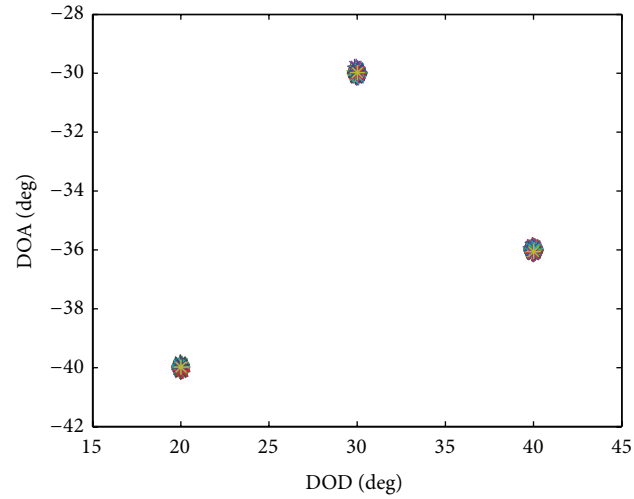

Figure 2: Angle estimation results with SNR = 15 dB.

effectively [20]. It is observed that the proposed algorithm performs slightly worse than the U-ESPRIT algorithm does in the DOD estimation in despite of the dramatic reduction in computational complexity (where the number of transmit antenna is $M = 8$ and the number of transmit beam is $L_t = 5 < M$). And the proposed algorithm and U-ESPRIT algorithm both have similar estimation performance of DOA due to the fact that the number of receiving beam is nearly equal to the number of transmitting antenna (where $L_r = 5$ and $N = 6$). Compared with the E-ESPRIT algorithm, although the beamspace unitary ESPRIT algorithm is a unitary algorithm, its performance will also be degraded because of the dramatic reduction in computational complexity. When the degradation is not large enough, the proposed algorithm also has a better performance over the element ESPRIT.

Figures 6 and 7 present the angle estimation performance of the proposed algorithm with different J, where $M = 8$, $N = 6$. The proposed algorithm is compared with the unitary ESPRIT algorithm. It illustrates that the angle estimation performance of our algorithm is improved as the number of snapshots increases. Meanwhile, it shows that performance of our algorithm is slightly worse than the unitary ESPRIT algorithm when the computational complexity is reduced all at once.

In Figure 8, values of transmitting array antennas $M = 6, 8$ and 10 ($N = 6$, $J = 64$) are examined for the SNR support. From Figure 8, it can be seen that the angle estimation performance of proposed algorithm will gradually increase with the increasing transmitting antenna number.

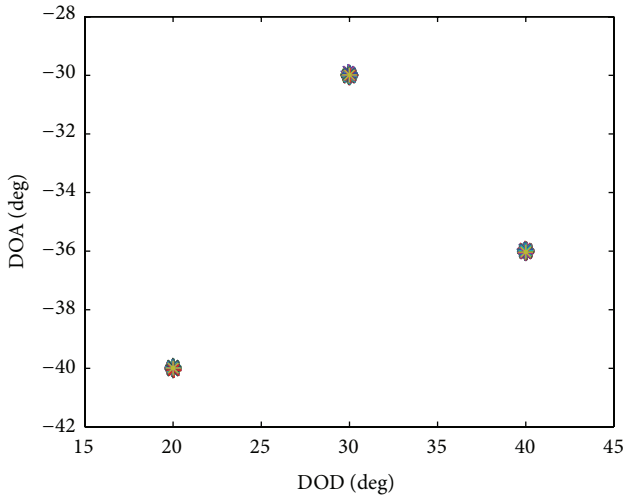

Figure 3: Angle estimation results with SNR = 20 dB.

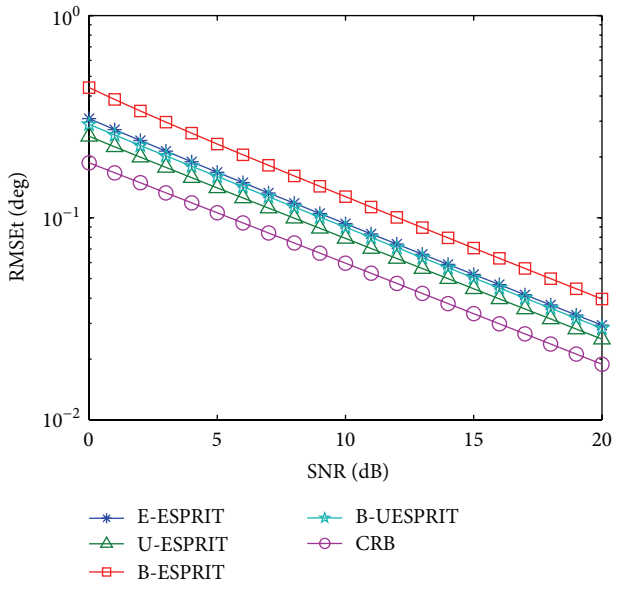

Figure 4: DOD estimation performance comparison.

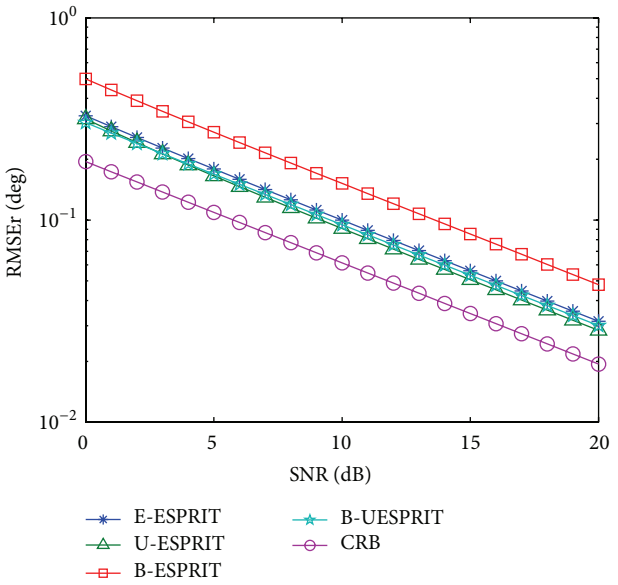

Figure 5: DOA estimation performance comparison.

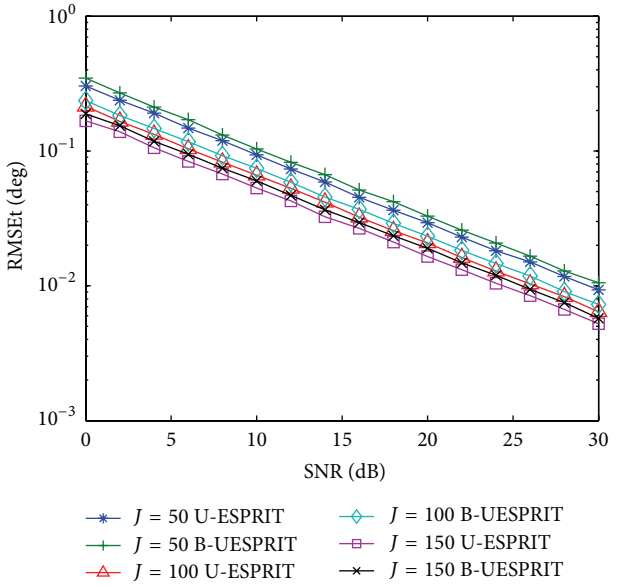

Figure 6: RMSE of DOD versus SNR for 3 sources with different values of sample.

Figure 9 gives the resolution performance of the proposed algorithm, the beamspace ESPRIT algorithm, the element ESPRIT algorithm, and the unitary ESPRIT algorithm. Considering a scenario with two uncorrelated sources of equal power, the angle parameters are $\theta_1 = \varphi_1 = -\delta/\sqrt{2}$ and $\theta_2 = \varphi_2 = \delta/\sqrt{2}$, and $J = 50$, SNR = 20 dB. Then the angular source separation is parameterized by [21]

$$2\delta = \sqrt{(\theta_1 - \theta_2)^2 + (\varphi_1 - \varphi_2)^2}. \quad (23)$$

The two sources are considered as resolved if the estimation of angle is close to the true angle parameter; that is,

$$\left(\widehat{\theta}_1 - \theta_1\right)^2 + \left(\widehat{\varphi}_1 - \varphi_1\right)^2 < \delta^2 \cap \left(\widehat{\theta}_2 - \theta_2\right)^2 + \left(\widehat{\varphi}_2 - \varphi_2\right)^2 < \delta^2. \quad (24)$$

It can be seen that the probability of resolution of proposed algorithm is better than both the beamspace ESPRIT algorithm and the element ESPRIT algorithm but slightly worse than the unitary ESPRIT algorithm.

Figure 10 depicts an evaluation of the computational complexity using TIC and TOC instructions that can serve for calculating the runtime of an algorithm in MATLAB. It can be seen that when all the beams are formed, the runtime of proposed algorithm is smaller than the U-ESPRIT algorithm in the case of the number of sensors is larger than 10. And when only five beams are formed, the runtime of proposed algorithm is much smaller than the U-ESPRIT

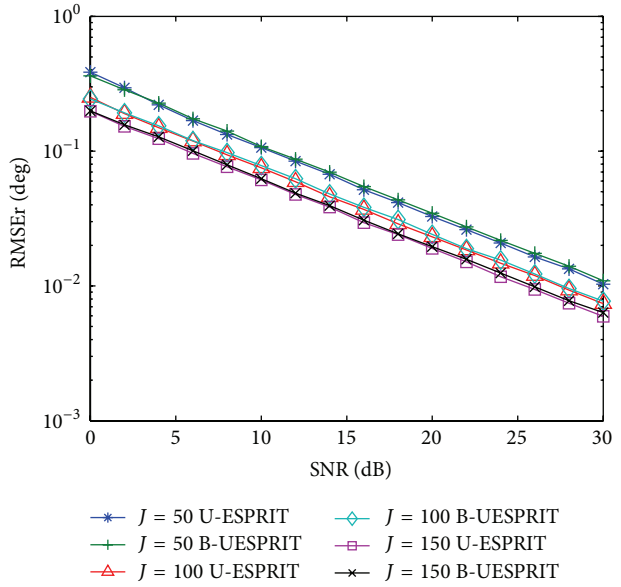

Figure 7: RMSE of DOA versus SNR for 3 sources with different values of sample.

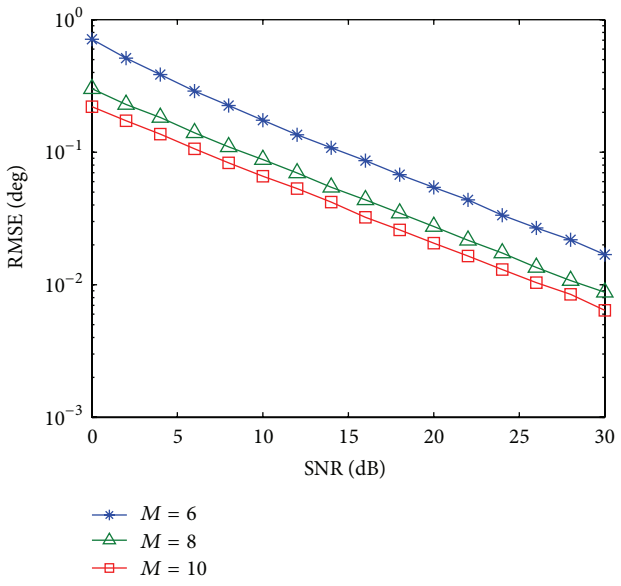

Figure 8: Total RMSE versus SNR for 3 sources with different values of M.

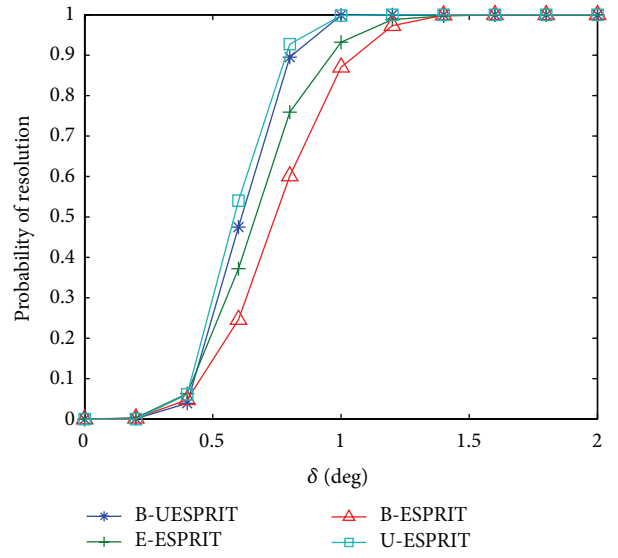

Figure 9: Probability of resolution versus angular separation δ, at SNR = 20 dB, $J = 50$.

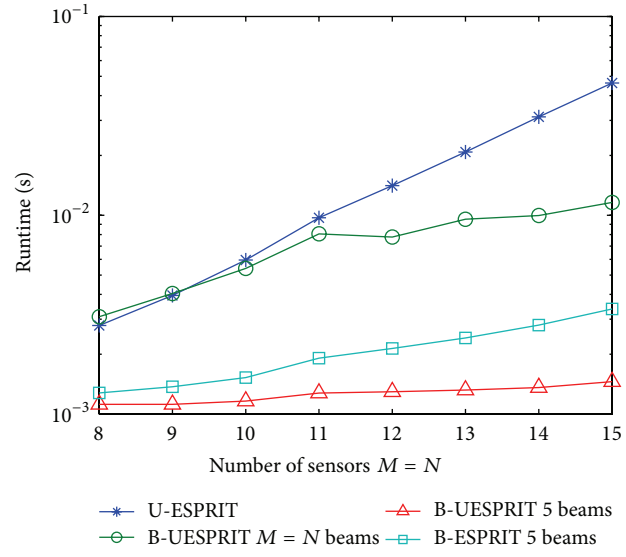

Figure 10: Runtime comparison against number of sensors $M = N$.

algorithm. Also, the runtime of the B-UESPRIT is smaller than the B-ESPRIT algorithm, which is still in the case of only five beams are formed. It is observed that as the number of sensors increases, the runtime of the proposed algorithm increases slowly. The reason is that the computational complexities and runtime of proposed algorithm are influenced by the number of beams formed, which is still five.

6. Conclusion

In this paper, a beamspace unitary ESPRIT is developed to estimate angles of the targets in bistatic MIMO radar. The conjugate centrosymmetrized DFT matrix is applied to transform the received data into beamspace. Then the invariance property of the transmitting beam and the receiving beam is exploited, respectively, to calculate the DODs and the DOAs of targets. Unlike the beamspace ESPRIT, the B-UESPRIT involves only real-valued computation from beginning to end. Therefore, a reduction of the computational complexity is obtained, which is demonstrated by the analysis of computational complexity and the runtime of algorithm. Furthermore, the simulation results prove that the B-UESPRIT requires no matched pair but possesses better angle estimation performance than the E-ESPRIT and the B-ESPRIT. Additionally, the CRB has been derived to analyze the performance.

Conflict of Interests

The authors declare that there is no conflict of interests regarding the publication of this paper.

References

[1] E. Fishler, A. Haimovich, R. Blum, D. Chizhik, L. Cimini, and R. Valenzuela, "MIMO radar: an idea whose time has come," in *Proceedings of the IEEE Radar Conference*, pp. 71–78, Philadelphia, Pa, USA, April 2004.

[2] I. Bekkerman and J. Tabrikian, "Target detection and localization using MIMO radars and sonars," *IEEE Transactions on Signal Processing*, vol. 54, no. 10, pp. 3873–3883, 2006.

[3] E. Fishler, A. Haimovich, R. S. Blum, L. J. Cimini Jr., D. Chizhik, and R. A. Valenzuela, "Spatial diversity in radars—models and detection performance," *IEEE Transactions on Signal Processing*, vol. 54, no. 3, pp. 823–838, 2006.

[4] A. M. Haimovich, R. S. Blum, and L. J. Cimini, "MIMO radar with widely separated antennas," *IEEE Signal Processing Magazine*, vol. 25, no. 1, pp. 116–129, 2008.

[5] J. Li and P. Stoica, "MIMO radar—diversity means superiority," in *Proceedings of the 14th Adaptive Sensor Array Process Workshop (ASAP '06)*, pp. 1–64, Lexington, Mass, USA, December 2006.

[6] J. Li and P. Stoica, "MIMO radar with colocated antennas," *IEEE Signal Processing Magazine*, vol. 24, no. 5, pp. 106–114, 2007.

[7] H. Yan, J. Li, and G. Liao, "Multitarget identification and localization using bistatic MIMO radar systems," *EURASIP Journal on Advances in Signal Processing*, vol. 2008, Article ID 283483, 2008.

[8] R. Xie, Z. Liu, and Z.-J. Zhang, "DOA estimation for monostatic MIMO radar using polynomial rooting," *Signal Processing*, vol. 90, no. 12, pp. 3284–3288, 2010.

[9] J. Li, P. Stoica, L. Xu, and W. Roberts, "On parameter identifiability of MIMO radar," *IEEE Signal Processing Letters*, vol. 14, no. 12, pp. 968–971, 2007.

[10] M. Jin, G. Liao, and J. Li, "Joint DOD and DOA estimation for bistatic MIMO radar," *Signal Processing*, vol. 89, no. 2, pp. 244–251, 2009.

[11] L. Xu, J. Li, and P. Stoica, "Target detection and parameter estimation for MIMO radar systems," *IEEE Transactions on Aerospace and Electronic Systems*, vol. 44, no. 3, pp. 927–939, 2008.

[12] X. Gao, X. Zhang, G. Feng, Z. Wang, and D. Xu, "On the MUSIC-derived approaches of angle estimation for bistatic MIMO radar," in *Proceedings of the International Conference on Wireless Networks and Information Systems (WNIS '09)*, pp. 343–346, December 2009.

[13] A. Zahernia, M. J. Dehghani, and R. Javidan, "MUSIC algorithm for DOA estimation using MIMO arrays," in *Proceedings of the 6th International Conference on Telecommunication Systems, Services, and Applications (TSSA '11)*, pp. 149–153, October 2011.

[14] C. Duofang, C. Baixiao, and Q. Guodong, "Angle estimation using ESPRIT in MIMO radar," *Electronics Letters*, vol. 44, no. 12, pp. 770–771, 2008.

[15] G. Zheng, B. Chen, and M. Yang, "Unitary ESPRIT algorithm for bistatic MIMO radar," *Electronics Letters*, vol. 48, no. 3, pp. 179–181, 2012.

[16] Y. D. Guo, Y. S. Zhang, and N. N. Tong, "Beamspace ESPRIT algorithm for bistatic MIMO radar," *Electronics Letters*, vol. 47, no. 15, pp. 876–878, 2011.

[17] M. D. Zoltowski, M. Haardt, and C. P. Mathews, "Closed-form 2D angle estimation with rectangular arrays via DFT beamspace ESPRIT," in *Proceedings of the 28th Asilomar IEEE Conference on Signals, Systems, and Computers*, pp. 682–687, 1994.

[18] M. D. Zoltowski, M. Haardt, and C. P. Mathews, "Closed-form 2-D angle estimation with rectangular arrays in element space or beamspace via unitary ESPRIT," *IEEE Transactions on Signal Processing*, vol. 44, no. 2, pp. 316–328, 1996.

[19] G. Xu, R. H. Roy III, and T. Kailath, "Detection of number of sources via exploitation of centro-symmetry property," *IEEE Transactions on Signal Processing*, vol. 42, no. 1, pp. 102–112, 1994.

[20] M. Haardt and J. A. Nossek, "Unitary ESPRIT: how to obtain increased estimation accuracy with a reduced computational burden," *IEEE Transactions on Signal Processing*, vol. 43, no. 5, pp. 1232–1242, 1995.

[21] P. Heidenreich, A. M. Zoubir, and M. Rübsamen, "Joint 2-D DOA estimation and phase calibration for uniform rectangular arrays," *IEEE Transactions on Signal Processing*, vol. 60, no. 9, pp. 4683–4693, 2012.